HHS Public Access

Author manuscript

Bioconjug Chem. Author manuscript; available in PMC 2021 February 19.

Published in final edited form as:

Bioconjug Chem. 2020 February 19; 31(2): 303–314. doi:10.1021/acs.bioconjchem.9b00669.

Recent advances in molecular imaging with gold nanoparticles

Mathilde Bouché[†], **Jessica C. Hsu**[†,§], **Yuxi C. Dong**[†,§], **Johoon Kim**[†,§], **Kimberly Taing**[†], **David P. Cormode**[†,§,*]

[†]Department of Radiology, University of Pennsylvania, Philadelphia, Pennsylvania 19104, United States

[§]Department of Bioengineering, University of Pennsylvania, Philadelphia, Pennsylvania 19104, United States

Abstract

Gold nanoparticles (AuNP) have been extensively developed as contrast agents, theranostic platforms and probes for molecular imaging. This popularity has yielded a large number of AuNP designs that vary in size, shape, surface functionalization and assembly, to match very closely to the requirements for various imaging applications. Hence, AuNP based probes for molecular imaging allow the use of computed tomography (CT), fluorescence and other forms of optical imaging, photoacoustic imaging (PAI) and magnetic resonance imaging (MRI), and other newer techniques. The unique physico-chemical properties, biocompatibility and highly developed chemistry of AuNP have facilitated breakthroughs in molecular imaging that allow the detection and imaging of physiological processes with a high sensitivity and spatial resolution. In this review, we summarize the recent advances in molecular imaging achieved using novel AuNP structures, cell tracking using AuNP, targeted AuNP for cancer imaging, and activatable AuNP probes. Finally, the perspectives and current limitations for the clinical translation of AuNP based probes are discussed.

Graphical Abstract

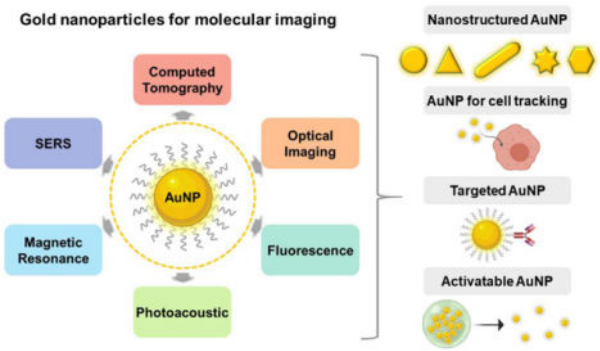

[*]Corresponding Author: Contact information: 3400 Spruce St, 1 Silverstein, Philadelphia, PA 19104, USA, Tel: 215-615-4656, Fax: 240-368-8096, David.Cormode@pennmedicine.upenn.edu.

Keywords

Gold nanoparticles; molecular imaging

Introduction

Imaging physiological and pathological processes for the early detection of a disease can greatly improve patient outcomes by providing key information on the disease characteristics or patients' response to treatments. To address this goal, a wide variety of novel probes for molecular imaging has been investigated, ranging from small molecules[1] to nanoparticles[2] and medical devices.[3] In particular, gold nanoparticles (AuNP) have shown great promises as imaging probes thanks to their ease of preparation, high stability in aqueous media, biocompatibility, and ability to provide strong contrast enhancement in multiple imaging modalities.[4,5]

Computed tomography (CT) is a standard imaging modality used routinely in clinics owing to its fast operation time, low cost and high spatial resolution.[6] This technique is based on the measurement of X-ray transmission through the subject, and the tissue dependent attenuation rate that can be reconstructed as 3D images, thus providing an anatomical representation of the subject. However, imaging soft tissues can be challenging unless using a contrast agent; iodinated molecules are typically used as standard of care.[7] AuNP have been found to be promising alternatives to the commercially available CT contrast agents by offering possibilities such as stronger contrast, increased circulation time or disease specific imaging.[8,9]

Fluorescence imaging relies on the sequential irradiation of the sample and delayed photon emission from the probe.[10] The high sensitivity, resolution and low cost render this technique popular for the semi-quantitative analysis of samples, although its low depth penetration is a limitation. AuNP based contrast agents in fluorescence imaging mostly encompass intrinsically fluorescent nanoclusters[11–13] or AuNP conjugated to a fluorescent dye that take advantage of the distance dependent quenching of fluorescence.[14]

Photoacoustic imaging (PAI) is a hybrid modality benefiting from the high acoustic resolution of ultrasound, and a high optical contrast at greater depth than other optical modalities.[15] In addition to being inexpensive, fast to operate and providing anatomical information in real time, this imaging modality is non-invasive and does not use ionizing radiation. Gold nanorods, gold nanoclusters and other AuNP based nanostructures have recently received growing interest for use as contrast agents in PAI, thanks to their tunable plasmonic absorbance that is capable of reaching the NIR.[16–18]

Magnetic resonance imaging (MRI) is a common imaging modality in clinical settings where the alignment of protons in water molecules is induced by a magnetic field pulse and the radiowaves released upon proton relaxation to the ground state are recorded and reconstructed as volumetric images.[19] MRI can be operated using either T_1 weighted or T_2 weighted sequences, depending on the tissue to be imaged and the diagnostic objectives. Although this technique requires longer acquisition time than CT or optical imaging, it

offers high soft tissue contrast. A large range of T_1 and T_2 contrast agents, creating positive or negative contrast respectively, have been developed for molecular imaging.[20,21] AuNP usually serve as carriers for paramagnetic metal complexes such as gadolinium,[22] or are combined with superparamagnetic materials such as Fe_3O_4 particles.[23]

More recently, AuNP based nanoprobes have also been designed to access molecular imaging using other imaging modalities such as surface-enhanced Raman scattering (SERS),[24] dark field microscopy (DFM), optical coherence tomography (OCT)[25] and so forth, although those modalities remain comparatively underexplored.

This review summarizes the challenges and possibilities in the design of gold nanoparticles for molecular imaging in cells and living systems. Focusing on developments over the past five years, we will cover the achievements in molecular imaging permitted by AuNP of various shapes, including spheres, rods, stars and so forth. Then, AuNP engineering for *in vivo* cell tracking will be discussed. The surface functionalization of AuNP for passive and active targeting of diseased sites and molecular imaging will be reviewed. Furthermore, we will cover activatable probes that change their contrast upon reaction with biomolecules of interest. Finally, the progress toward clinical translation of AuNP probes will be discussed.

Types of gold nanoparticles

AuNP are commonly obtained by reduction of a gold salt, and coated in an organic[26] or inorganic[27] layer to provide colloidal stability. AuNP are characterized by a localized surface plasmon resonance (LSPR), which is due to the collective oscillations of the free electrons along the gold lattices in the AuNP core.[28] This LSPR can be finely tuned to access desired optical properties *via* different sizes, shapes, coatings and assemblies of AuNP. Since the seminal work by Turkevich on the synthesis of spherical AuNP,[29] a large array of adapted procedures has been reported that adjust the reaction conditions to vary the sizes of spherical AuNP.[30,31] Modification of the size of AuNP is of particular interest for molecular imaging, owing to the greater surface to core ratio available for conjugation of targeting moieties or dyes. Moreover, increasing the size of AuNP induces a bathochromic shift of their LSPR, which can be beneficial since many optical biomedical techniques are performed in the near-infrared region (NIR), *i.e.* 650–900 nm, a part of the spectrum where the absorption of tissue is low.[32] On the other hand, the surface to core ratio has no effect on the contrast enhancement achieved in CT, and instead affects the pharmacokinetics and biodistribution of AuNP, thus granting their utility for different applications in molecular imaging.[33]

Shape variations of AuNP

Procedures have been developed to synthesize AuNP in various shapes. For example, gold nanorods (AuNR) have the significant advantage of possessing both transverse and longitudinal LSPRs that can be shifted to the NIR by adjusting the length-to-width ratio.[34] Interestingly, miniature AuNR have been reported whose LSPR absorbs in the NIR-II, *i.e.* beyond 900 nm.[35] These miniature AuNR allowed a 30 % improvement in tumor accumulation, and 4.5 fold enhancement in the PAI contrast in tumor imaging compared to larger AuNR. Core-shell AuNR have also been developed that are effective contrast agents

for multiple modalities.[36] Notably, a spindle-shaped iron oxide core that offers T_2 contrast in MRI was covered in a gold shell to yield a probe referred to as 'nanorice', that allowed multimodal imaging by MRI, PAI in the NIR and SERS.[37] Other original shape variations have been developed to finetune both the optical properties and cellular uptake of AuNP, such as prisms, stars and triangles.[38] The strong light scattering properties of gold nanoprisms make them valuable contrast agents for imaging the microvasculature in skin or in melanoma tumors using OCT.[39] Stars provide a high surface to core ratio which is advantageous for surface functionalization with targeting ligands, and allow molecular imaging with SERS,[40,41] or CT.[42] Furthermore, the effect of the shape of AuNP on their accumulation in RAW264.7 macrophages was evaluated comparing stars, prisms and triangles. Lin et al. showed triangles accumulate to a larger extent into RAW264.7 macrophages compared to other shapes, thus allowing higher local contrast enhancement for their imaging.[38]

Assemblies of AuNP

Assembling AuNP in close proximity of each other induces interparticle plasmon coupling and shifts their absorption to the NIR.[28] To produce AuNP assemblies, inorganic nanomaterials such iron oxide nanoparticles (IONP), which provide T_2 weighted MR contrast, can be used as a template to enable multimodality imaging.[43] Similarly, a variety of liposomes, micelles and polymers have been used to assemble AuNP and other imaging agents into one multifunctional nanoplatform.[44,45] Recently, biodegradable assemblies of AuNP have received significant interest for their contrast generating properties while potentially allowing their degradation and clearance. Cheheltani et al. encapsulated sub-5 nm hydrophilic AuNP in larger biodegradable PCPP nanospheres to form an agent termed Au-PCPP (Figure 1A), which provided significant contrast enhancement in CT (Figure 1B) and PAI (Figure 1C).[9] Moreover, the intrinsic biodegradability of the PCPP polymer was shown to grant the release of single AuNP upon degradation of the nanospheres (Figure 1D). Furthermore, other biodegradable polymers, such as PLGA, can be used to form assemblies with AuNP for tumor imaging by a combination of PAI and CT.[46,47]

An alternative approach to access AuNP assemblies that provide significant contrast enhancement for molecular imaging, while having intrinsic biocompatibility and beneficial pharmacological properties, relies on the use of biomimetic coatings.[48] Sun et al. assembled multiple gold nanoclusters within a ferritin nanocage for passive targeting of kidneys, thus allowing their *in vivo* fluorescence imaging that was corroborated by the higher gold content found in the kidneys compared to other major organs.[49] AuNP templating along the fibrils of human islet amyloid polypeptide can also be achieved *in situ* by bioreduction of a gold precursor, thus allowing their imaging.[50] Moreover, AuNP can be assembled in cell membranes derived from red blood cells (RBC), platelets and cancer cells.[51,52] For example, Li et al. showed the self-assembly of pea protein isolate (PPI) and NIR fluorescent gold nanoclusters (AuNCs) into hybrids (AuNCs/PPI NPs), which could be encapsulated in RBC membranes (AuNCs/PPI@RBC), and intravenously injected into tumor-bearing mice for *in vivo* optical imaging (Figure 2A).[53] The core size of AuNCs/PPI NPs (Figure 2B), of approximately 100 nm, was found unchanged upon fusion with RBC membrane (Figure 2C). Stronger NIR fluorescence intensity at the tumor site was observed with RBC-coated

nanoparticles (Figure 2D), suggesting that RBC coating can effectively avoid uptake by phagocytic cells and grant tumor imaging by enhanced tumor accumulation thanks to longer blood circulation. Furthermore, others have shown the *in situ* synthesis of AuNP in living platelets using ultrasound, and demonstrated their contrast properties *in vitro* by CT and PAI.[54,55]

Overall, AuNP of a wide range of sizes, shapes and coatings can be engineered to change their pharmacological properties and contrast generation to meet with the requirements of molecular imaging. However, their long-term retention, biodegradation and safety profiles will have to be thoroughly evaluated to understand their *in vivo* behaviors and side effects. In the coming decade, we expect to see more progress made in engineering biomimetic AuNP with new functions and specialized coatings such as cancer cell membranes, membrane proteins, targeting ligands or combinations of different membrane types.

Gold nanoparticles for cell tracking

Fine-tuning the physico-chemical properties of AuNP can also be exploited for optimizing the probe loading for cell tracking in evaluation of cell-based therapies. Such therapies might offer a better treatment option for diseases where conventional therapeutic approaches, such as oncology and regenerative medicine, have shown limitations.[56] The most widely used cell types in cell-based therapies are stem cells for regenerative medicine, and genetically reprogrammed immune cells for immunotherapy.[56–59] In both cases, it is important that the administered cells migrate, home, and maintain their functionalities at the site of interest for prolonged therapeutic efficacy. However, so far the outcome of human clinical trials using such therapies have been mixed, partially due to the shortcomings of currently used monitoring techniques, such as histopathology and *ex vivo* biomarker analyses.[56,59,60] These techniques often require invasive procedures and provide incomplete information on the cell fate in the *in vivo* environment. Direct monitoring by cell tracking has been highlighted as a novel method to better understand the behavior of the transplanted cells, such as migration and distribution.[61–63] Cell tracking can provide this valuable information in a noninvasive and real-time manner that can be used to adjust cell type, dose, and administration route for optimal therapeutic efficacy and safety profile. Various noninvasive imaging modalities are used to track and monitor cells after transplantation, and cell tracking using AuNP has been studied with CT imaging.[64] *Ex vivo* direct labeling is most commonly used for cell tracking with AuNP. In this approach, the target cells are incubated with AuNP *in vitro* prior to transplantation, allowing AuNP to be internalized in the cells. Both the beneficial biocompatibility and the high elemental density of gold in AuNP are advantageous for CT cell tracking to maximize the local payload concentration due to the relatively low sensitivity of CT, while minimally disrupting the cell viability and function.

An abundance of previous studies has demonstrated the significance of physiochemical parameters of AuNP, such as size, shape, and surface chemistry, in maximizing their cellular uptake with minimal cell impairment.[65–68] A recent study by Chhour et al. investigated the effect of size and surface chemistry in AuNP uptake by monocytes.[69] The effect of both the coating and the size of AuNP on their cellular uptake was evidenced using AuNP

formulations with core diameter ranging from 15 to 150 nm and functionalized with various organic coatings. AuNP formulations with methoxy-PEG coatings showed greater uptake with increasing diameter, while coating with PEG bearing a terminal carboxylic group induced a maximized uptake for formulations of 50 and 75 nm rather than smaller or larger diameters. The time of incubation and concentration of AuNP are also important considerations for the optimization of cell tracking as demonstrated by Betzer et al. using glucose-coated, 20 nm diameter AuNP.[70] Another study by Sun et al. further demonstrated the importance in considering the dependence of cellular uptake on nanoparticle formulations, labeling parameters, and cell types.[71] Moreover, recent studies have also emphasized the effect of serum protein corona on nanoparticle-cell interaction and further internalization.[72–74] The nature of protein coronas is directed by both the size and surface chemistry of AuNP and accordingly changes their cellular uptake.[75–77] Therefore, considering the variability among findings of previous studies and the large number of parameters to review, it is essential to investigate the best AuNP formulation and optimize the labeling conditions for each cell tracking application. The synthetic control over AuNP morphology (*i.e.* size and shape) and their extensive surface modification possibilities make their optimization for specific applications more facile.

With better understanding of AuNP uptake in various cell types, many studies have used selected AuNP formulations to demonstrate tracking of non-phagocytic cells upon labelling in small animals using CT imaging.[78–81] In a recent study, Kim et al. coated 40 nm in diameter AuNP with poly-l-lysine (PLL), covalently functionalized with the rhodamine B isothiocyanate (RITC) dye, to monitor human mesenchymal stem cells (hMSCs) in rat brains (Figure 3A,B).[82] Owing to the well-established role of PLL as a cationic transfection agent, the labeling efficiency of smaller and non-phagocytic hMSCs was improved using PLL coated AuNP (AuNP-PLL), at gold concentration of 0.2 $mg.mL^{-1}$ and upon 12 hours of incubation (Figure 3C). Hence, labeling hMSC with AuNP-PLL reached more than 600 pg/cell and did not impair cell viability, proliferation, or differentiation capabilities. Suspension of those labeled hMSCs produced strong attenuation in CT imaging that was linearly proportional to the concentration of internalized AuNP (Figure 3D). Transplants containing as low as 2×10^5 cells could be visualized with CT in rat brains (Figure 3E) and confirmed by immunofluorescence microscopy thanks to the RITC functionalized AuNP (Figure 3F). In the case of primary human T-cells that are genetically engineered against melanoma-specific T-cell receptors, Meir et al. used glucose coating to enhance the labelling efficiency of 20 nm AuNP.[83] Optimal *in vivo* labeling conditions of 60 minutes incubation time at gold treatment concentration of 0.75 $mg.mL^{-1}$ did not significantly impair the labeled cells' function or viability. After intravenous injection into tumor-bearing mice of 16×10^6 of the labeled cells, distinct CT attenuation was observed at the tumor site as early as 24 hours.

The use of AuNP as probes for cell tracking is not limited to CT imaging, and engineered AuNP have been effectively visualized upon cell internalization with other imaging modalities, such as photoacoustic imaging.[35] For instance, Comenge et al. recently demonstrated the tracking of mesenchymal stem cells that were labeled with gold nanorods using PAI.[84] Alternatively, by incorporating radionuclides on AuNP before cell labeling, cell tracking with radionuclide imaging can be performed as well. Lee et al. demonstrated the

feasibility of cell tracking via PET imaging with radiolabeled AuNP, using dendritic cells labelled with core-shell AuNP incorporating iodine-124.[85] Optical coherence tomography can also be used for tracking in living systems circulating tumor cells that were labelled with gold nanorods.[86]

AuNP have advantageous features for cell tracking with CT owing to their high density, biocompatibility, X-ray attenuation properties and the large array of AuNP shape and surface functionalization, and therefore have been the focus of numerous studies using CT to monitor cell-based therapies. However, recent studies suggest the possibility of cell tracking with AuNP probes for photon-counting CT, which can provide additional benefits to CT cell tracking, such as specific visualization of contrast generated from AuNP and non-invasive AuNP quantification with high accuracy.[87,88]

Targeted gold nanoparticles based nanoprobes

Passively targeted AuNP

The unique pathophysiological properties and structures of the tumor tissue, *i.e.* the "leaky" tumor vasculature and impaired lymphatic drainage, allow the passive targeting of tumors by AuNP thanks to the enhanced permeability and retention (EPR) effect.[89–91] Enhanced retention of AuNP with appropriate sizes and coatings is advantageous for tumor imaging and cancer detection.[92–94] Ashton et al. evidenced such passive targeting with spherical PEG coated AuNP of 29.9 nm hydrodynamic diameter, that were injected into mice bearing primary lung tumors.[95] Sykes et al. observed different tumor accumulation profiles in a breast cancer model when studying AuNP ranging in size from 15–100 nm, with the highest AuNP tumor accumulation occurring for the AuNP that had the smallest diameter.[96] This is likely due in part to the longer circulation half-lives of smaller AuNP, thus enhancing the probability of AuNP entering the tumor from the blood.[97] Moreover, small AuNP have been used for brain tumor imaging *via* passive targeting.[98,99] Hence, Smilowitz et al. suggested that AuNP intravenously injected can effectively accumulate in both an intracerebral main tumor mass and migrated tumor cells, thus having potential for imaging glioblastoma.[100] In addition to size, the shape and surface chemistry of AuNP significantly affect their distribution and cell uptake,[9,38,101,102] and accordingly play important roles in passive tumor-targeting efficacy.[103] Modification of AuNP with PEG coating has been extensively investigated to enhance their blood circulation time and thus the EPR effect to facilitate tissue-specific imaging.[104–106] For instance, PEG-AuNP show a 3-fold higher concentration in blood and greater tumor accumulation 3 hours after intravenous injection for tumor imaging with CT, compared to tiopronin coated AuNP.[107] Furthermore, passive targeting of AuNP in the tumor is valuable to access multi-modality imaging (*e.g.* CT and PAI) for both tumor imaging and image guided therapy.[108–111]

Actively targeted AuNP

As opposed to passive targeting, active targeting is achieved by functionalizing the surface of AuNP with molecules that specifically bind to cell surfaces or other biomolecules.[112,113] Actively targeted AuNP are expected to strongly interact upon encountering their target *in vivo*, therefore directing AuNP to pathological sites by other mechanisms in addition to the

EPR effect. Conjugating cell receptor targeting moieties to AuNP based probes has received extensive interest for cancer imaging, and therefore a large variety of targeting ligands has been investigated, such as cetuximab (C225) to target epidermal growth factor receptor (EGFR), herceptin to target the human epidermal growth factor receptor 2 (HER2),[114,115] and so forth.[116] Alternatively, AuNP coated with hyaluronic acid (HA) and manganese chelates that take advantage of the inherent CD44 receptor targeting ability of HA, granted tumor imaging by CT and MR dual-mode imaging.[117] Moreover, Dinish et al. reported AuNP labeled with NIR active organic molecules and targeted with anti-EGFR antibodies, which could image cancer by bimodal PAI and SERS imaging (Figure 4).[118] Peptide coated AuNP have found broad application in the field of molecular imaging and image guided therapy for photodynamic therapy of tumors, optical and CT imaging of thrombus, and so forth.[119–121] Notably, Avvakumova et al. developed gold nanocages conjugated to neuropeptide Y (NPY) for image guided photothermal therapy of prostate tumor.[122] Peptide functionalized AuNP can also be used for targeting and imaging tumor-associated macrophages (TAMs) and lung cancer cells by CT.[123] Furthermore, glycol-chitosan-coated AuNP appended with fibrin-binding peptides enabled the detection of cerebrovascular thrombi.[124]

In summary, thanks to the intense research interest on targeted AuNP as probes for molecular imaging and disease detection, a large array of variations has been reported to adapt the imaging properties to the requirements of multiple diseases. By strategically controlling the physical properties and surface functionalization of AuNP, both passive and active targeting strategies can be accessed for molecular imaging, and has found additional applications for image guided therapy.

Activatable AuNP based nanoprobes

Aiming at enhancing the probes' selectivity for molecular imaging, the concept of activatable probes has bloomed, encompassing careful engineering to locally change the probe's imaging signal as a response to biomolecules.[125–127] This signal switch improves the diagnostic's specificity and precision by enabling visualization of biomolecules and pathological phenomena.[128] The broad possibilities for the surface modification of AuNP, and the variety of available responsive motifs, render activatable nanoparticles promising probes for molecular imaging.[129]

Distance dependent fluorescence quenching of AuNP functionalized with dyes

Owing to the optical properties of AuNP, they can act as dark quenchers for fluorescent moieties located close to the metal core.[130] Therefore, AuNP conjugated with a fluorescent moiety through a biomolecule-responsive linker allow the specific and local release of the dye for turning-on the probe's signal in fluorescence imaging. This concept has been used to image a wide array of biomolecules with AuNP based nanoprobes, namely pH,[131,132] ROS,[133,134] proteins,[135] enzymes,[136,137] RNA,[138–140] metal ions,[141,142] and other metabolites.[143,144] Intracellular pH regulation is critical to living cells and can be used as one of the hallmarks of cancer metabolism for early diagnosis.[145] Recently, several studies have demonstrated the possibility of imaging pH variations at the cellular level using engineered

AuNP based nanoprobes.[146–149] For example, Yu et al. constructed a pH-sensitive AuNP functionalized with fluorescent dyes, one responsive to acidic pH and the other to basic pH, and such a system can be used for mapping brain pH variations very finely using fluorescence imaging.[150] Notably, Kwon et al. reported the use of silica coated AuNP functionalized with a thrombin-cleavable fluorescent peptide as an activatable probe for bimodal thrombus imaging in fluorescence and CT.[120] *In vitro*, the fluorescence increased by 30% upon thrombin exposure thanks to the probe activation. *In vivo*, the thrombus could be visualized both by thrombin triggered signal enhancement in fluorescence imaging, and by CT imaging thanks to the size dependent accumulation in the diseased area by EPR effect. Alternatively, a caspase responsive multicolor nanoprobe was developed for monitoring in real-time the mechanism of caspase cascade occurring during cell apoptosis.[151] In this aim, three different peptides, cleavable upon exposure to either caspase-3, −8 or −9, were functionalized on one end with three different fluorescent dyes, and conjugated to AuNP *via* their other end. This nanoprobe showed signal quenching in the absence of caspase, and effective caspase dependent signal turn-on in fluorescence, without interference from other biomolecules. Then, the sequential caspase activation on HeLa cells treated with staurosporine, an apoptosis inducer, could be visualized by fluorescence with high precision and selectivity, as a proof-of-concept for further drug mechanistic investigations.

Interparticle coupling in AuNP assemblies

The interparticle plasmon coupling that occurs when multiple AuNP are located in a close vicinity, induces bathochromic shift of their LSPR, potentially into the NIR, and can be reverted upon disassembly of the structure for the release of single AuNP.[28] This reversible behavior can be used in the development of activatable probes by biomolecule mediated assembly or disassembly, to change the imaging signal in the diseased area. Numerous synthetic strategies have been explored to access plasmonic assemblies of AuNP,[152,153] and used for drug delivery[154] or theranostic applications.[155,156] However, their use as probe for molecular imaging is less explored, and most studies focus on indirect biomolecule imaging by *in situ* AuNP aggregation triggered by the biomolecule of interest. Hence, Zn^{2+} ions that are involved in carcinogenesis and neural signaling, were imaged by zinc-induced peptide folding at the surface of AuNP, and triggered AuNP aggregation for indirect multiphoton-induced luminescence imaging of Zn^{2+}.[157] Similarly, pH changes associated with cancer were imaged by PAI thanks to the pH-induced protonation of the coating of AuNP and their subsequent electrostatic aggregation.[158] In order to image pH variations in brain tumors for image guided surgery, AuNP were coated with a gadolinium complex for MRI, a pH cleavable hydrazone modified PEG shielding coating, and an inner coating capable of *in vivo* copper-free click reaction to bind AuNP in clusters.[159] The pH triggered aggregation of AuNP in brain tumor allowed for the indirect pH imaging by signal enhancement in MRI as well as SERRS by interparticle ‘hotspot’ formation. This system was used as both preoperative agent for delimiting the tumor margins by MRI, and intraoperative tumor excision agent by bimodal MRI and SERRS imaging.

On the other hand, signal changes induced by *in situ* AuNP disassembly can be used for biomolecule imaging. For example, glutathione (GSH), a redox active biomolecule, can be imaged thanks to its ability to cleave a dithiol linker that forms an AuNP aggregate, resulting

in dis-aggregation of AuNP and turn-on of fluorescence.[160] Moreover, radical oxygen species (ROS), a hallmark of inflammation and cancer, could be imaged with ROS degradable AuNP-polyphosphazene nanoprobes due to loss of PA signal upon degradation (Figure 5A).[161] Sub-5 nm AuNP display strong PA signal thanks to interparticle plasmon coupling when loaded in the polyphosphazene spheres (Figure 5B), while their exposure to ROS induced polyphosphazene degradation (Figure 5C) and significantly decreased the PA signal. This activatable nanoprobe allowed ROS imaging by PA signal decrease in inflamed RAW264.7 macrophages, and differentiation from normal macrophages where the nanoprobes maintained a high PA contrast (Figure 5D,F). CT was used in combination with PAI to permit the imaging of endogenous ROS since its signal is dependent on the gold concentration and not affected by its environment (Figure 5E).

Metal etching in AuNP based inorganic composites

AuNP based molecular imaging can be achieved by designing core-shell particles and alloys, where a responsive shell covers the gold core and quenches its optical properties. Then, a biomolecule mediated galvanic exchange at the surface of the composites decreases the gold quenching for turning-on the signal in optical imaging. Hence, Au-Ag alloys were shown to etch upon cyanide exposure, therefore granting a cyanide detection in pollutes as low as 1 nM, in zebra fish.[162] Similarly, gold nanorods covered in silver were shown to etch in response to superoxide radicals ($O_2^{\bullet -}$), thus shifting the nanoprobe plasmon resonance scattering and allowing real-time imaging of $O_2^{\bullet -}$ and of the associated autophagy process.[163] Kim et al. have applied a similar principle using gold nanorods covered in a silver layer (Au/AgNR) as an activatable probe where the PA signal is quenched unless silver gets oxidized by ROS to release silver ions and restore the PA signal (Figure 6).[164] Such Au/AgNR could be used as a theranostic platform, allowing the simultaneous release of silver ions for antibacterial therapy in mice, in addition to self-report silver ion delivery in a non-invasive manner.

Overall, AuNR based activatable nanoprobes have shown significant progress in the field of molecular imaging, evolving toward more specific detection by signal change. Hence, the versatility of AuNP synthesis and the large range of designs available, has greatly advanced the field by using biomolecule responsive coatings or triggered assembly and disassembly processes to shift their optical properties. Yet, translation to clinical trials of activatable nanoprobes based on AuNP has yet to be explored.

Conclusion

Overall, significant development in the field of AuNP based probes has been achieved over the past five years, seeing more complex and specific probes appear. This intense development arises from the challenges in molecular imaging requiring the detection of biomolecules that are often present in disease sites at sub-millimolar concentrations, and despite the complex environment in living systems. In particular, AuNP based probes have shown remarkable results in molecular imaging both at the cellular level and as contrast agents for *in vivo* imaging. Although the research around AuNP based nanoprobes has bloomed over the timeline covered herein, only a small number of AuNP based biomaterials

are currently being investigated in clinical trials, notably AuroLase, and no AuNP has yet been approved for use in patient care.[165–167] This discrepancy between research interests and translation to human can in part be explained by the lack of comparable information related to their biodistribution, degradability, systemic toxicity and concerns related to their excretion profile and possible long-term accumulation in the body.[168] Accordingly, systematic investigation of such parameters using comparable techniques should greatly favor the better understanding of optimal physico-chemical and pharmacological parameters of AuNP for eventual clinical translation. While new technical developments in gold nanoparticle synthesis and use in imaging are welcome, it will be important for the field to focus more on clinical translation in the coming years. Excretion of gold nanoparticles will be key in most applications to achieve approval for clinical use, so the use of gold nanostructures that can be excreted (such as sub-5 nm AuNP or assemblies of such AuNP that can be degraded) should receive more attention in the future. Moreover, in this field, as in many others, clinical translation will be facilitated if researchers take care to obtain intellectual property on their agents, from companies to commercialize their agents and seek funding to gather investigational new drug status enabling data in order to proceed to clinical trials. In summary, in the next five years, we expect that there will be more exciting new discoveries, as well as more progress on clinical translation, to bring the benefits of gold nanoparticles to preclinical and clinical imaging.

Acknowledgements

We thank the Franco-American Commission Fulbright for fellowship support to M.B. This work was also supported by NIH (R01 HL131557 and R01 CA227142).

References

(1). Qiu KQ, Chen Y, Rees TW, Ji LN, and Chao H (2019) Organelle-targeting metal complexes: from molecular design to bio-applications. Coord. Chem. Rev 378, 66–86.

(2). Kunjachan S, Ehling J, Storm G, Kiessling F, and Lammers T (2015) Noninvasive imaging of nanomedicines and nanotheranostics: principles, progress, and prospects. Chem. Rev 115, 10907–10937. [PubMed: 26166537]

(3). Syedmoradi L, Daneshpour M, Alvandipour M, Gomez FA, Hajghassem H, and Omidfar K (2017) Point of care testing: the impact of nanotechnology. Biosens. Bioelectron 87, 373–387. [PubMed: 27589400]

(4). Elahi N, Kamali M, and Baghersad MH (2018) Recent biomedical applications of gold nanoparticles: a review. Talanta 184, 537–556. [PubMed: 29674080]

(5). Guo JF, Rahme K, He Y, Li LL, Holmes JD, and O'Driscoll CM (2017) Gold nanoparticles enlighten the future of cancer theranostics. Int. J. Nanomed 12, 6131–6152.

(6). Goldman LW (2007) Principles of CT and CT technology. J. Nucl. Med. Technol 35, 115–128. [PubMed: 17823453]

(7). Pasternak JJ, and Williamson EE (2012) Clinical pharmacology, uses, and adverse reactions of iodinated contrast agents: a primer for the non-radiologist. Mayo Clin. Proc 87, 390–402. [PubMed: 22469351]

(8). Bernstein AL, Dhanantwari A, Jurcova M, Cheheltani R, Naha PC, Ivanc T, Shefer E, and Cormode DP (2016) Improved sensitivity of computed tomography towards iodine and gold nanoparticle contrast agents via iterative reconstruction methods. Sci. Rep 6.

(9). Cheheltani R, Ezzibdeh RM, Chhour P, Pulaparthi K, Kim J, Jurcova M, Hsu JC, Blundell C, Litt HI, Ferrari VA, et al. (2016) Tunable, biodegradable gold nanoparticles as contrast agents for

computed tomography and photoacoustic imaging. Biomaterials 102, 87–97. [PubMed: 27322961]

(10). Lichtman JW, and Conchello JA (2005) Fluorescence microscopy. Nat. Methods 2, 910–919. [PubMed: 16299476]

(11). Qu XC, Li YC, Li L, Wang YR, Liang JN, and Liang JM (2015) Fluorescent gold nanoclusters: Synthesis and recent biological application. J. Nanomater

(12). Schaeffer N, Tan B, Dickinson C, Rosseinsky MJ, Laromaine A, McComb DW, Stevens MM, Wang YQ, Petit L, Barentin C, et al. (2008) Fluorescent or not? size-dependent fluorescence switching for polymer-stabilized gold clusters in the 1.1–1.7 nm size range. Chem. Commun, 3986–3988.

(13). Zhou C, Long M, Qin Y, Sun X, and Zheng J (2011) Luminescent gold nanoparticles with efficient renal clearance. Angew. Chem., Int. Ed 50, 3168–3172.

(14). Swierczewska M, Lee S, and Chen XY (2011) The design and application of fluorophore-gold nanoparticle activatable probes. Phys. Chem. Chem. Phys 13, 9929–9941. [PubMed: 21380462]

(15). Erfanzadeh M, and Zhu Q (2019) Photoacoustic imaging with low-cost sources; a review. J. Photoacoust 14, 1–11.

(16). Li WW, and Chen XY (2015) Gold nanoparticles for photoacoustic imaging. Nanomedicine 10, 299–320. [PubMed: 25600972]

(17). Liu YJ, Bhattarai P, Dai ZF, and Chen XY (2019) Photothermal therapy and photoacoustic imaging via nanotheranostics in fighting cancer. Chem. Soc. Rev 48, 2053–2108. [PubMed: 30259015]

(18). Jiang X, Du B, Tang S, Hsieh JT, and Zheng J (2019) Photoacoustic imaging of nanoparticle transport in the kidneys at high temporal resolution. Angew. Chem., Int. Ed 58, 5994–6000.

(19). Vijayalaxmi Fatahi M., and Speck O (2015) Magnetic resonance imaging (MRI): a review of genetic damage investigations. Mutat. Res., Rev. Mutat. Res 764, 51–63. [PubMed: 26041266]

(20). Ni DL, Bu WB, Ehlerding EB, Cai WB, and Shi JL (2017) Engineering of inorganic nanoparticles as magnetic resonance imaging contrast agents. Chem. Soc. Rev 46, 7438–7468. [PubMed: 29071327]

(21). Xiao YD, Paudel R, Liu J, Ma C, Zhang ZS, and Zhou SK (2016) MRI contrast agents: classification and application (review). Int. J. Mol. Med 38, 1319–1326. [PubMed: 27666161]

(22). Debouttiere PJ, Roux S, Vocanson F, Billotey C, Beuf O, Favre-Reguillon A, Lin Y, Pellet-Rostaing S, Lamartine R, Perriat P, et al. (2006) Design of gold nanoparticles for magnetic resonance imaging. Adv. Funct. Mater 16, 2330–2339.

(23). Sanchez A, Paredes KO, Ruiz-Cabello J, Martinez-Ruiz P, Pingarron JM, Villalonga R, and Filice M (2018) Hybrid decorated core@shell janus nanoparticles as a flexible platform for targeted multimodal molecular bioimaging of cancer. ACS Appl. Mater. Interfaces 10, 31032–31043. [PubMed: 30141615]

(24). Harmsen S, Huang RM, Wall MA, Karabeber H, Samii JM, Spaliviero M, White JR, Monette S, O'Connor R, Pitter KL, et al. (2015) Surface-enhanced resonance raman scattering nanostars for high-precision cancer imaging. Sci. Transl. Med 7.

(25). Liba O, SoRelle ED, Sen D, and de la Zerda A (2016) Contrast-enhanced optical coherence tomography with picomolar sensitivity for functional in vivo imaging. Sci. Rep 6, 23337. [PubMed: 26987475]

(26). Sun L, Joh DY, Al-Zaki A, Stangl M, Murty S, Davis JJ, Baunnann BC, Alonso-Basanta M, Kao GD, Tsourkas A, et al. (2016) Theranostic application of mixed gold and superparamagnetic iron oxide nanoparticle micelles in glioblastoma multiforme. J. Biomed. Nanotechnol 12, 347–356. [PubMed: 27305768]

(27). Moreira AF, Rodrigues CF, Reis CA, Costa EC, and Correia IJ (2018) Gold-core silica shell nanoparticles application in imaging and therapy: a review. Microporous Mesoporous Mater 270, 168–179.

(28). Amendola V, Pilot R, Frasconi M, Marago OM, and Iati MA (2017) Surface plasmon resonance in gold nanoparticles: a review. J. Phys.: Condens. Matter 29.

(29). Turkevich J, Stevenson PC, and Hillier J (1951) A study of the nucleation and growth processes in the synthesis of colloidal gold. Discuss. Faraday Soc, 55-&.

(30). Grzelczak M, Perez-Juste J, Mulvaney P, and Liz-Marzan LM (2008) Shape control in gold nanoparticle synthesis. Chem. Soc. Rev 37, 1783–1791. [PubMed: 18762828]

(31). Wall MA, Harmsen S, Pal S, Zhang LH, Arianna G, Lombardi JR, Drain CM, and Kircher MF (2017) Surfactant-free shape control of gold nanoparticles enabled by unified theoretical framework of nanocrystal synthesis. Adv. Mater 29.

(32). Maturi M, Locatelli E, Monaco I, and Franchini MC (2019) Current concepts in nanostructured contrast media development for in vivo photoacoustic imaging. Biomater. Sci 7, 1746–1775. [PubMed: 30901017]

(33). Dong YC, Hajfathalian M, Maidment PSN, Hsu JC, Naha PC, Si-Mohamed S, Breuilly M, Kim J, Chhour P, Douek P, et al. (2019) Effect of gold nanoparticle size on their properties as contrast agents for computed tomography. Sci. Rep 9, 14912. [PubMed: 31624285]

(34). Knights OB, Ye SJ, Ingram N, Freear S, and McLaughlan JR (2019) Optimising gold nanorods for photoacoustic imaging in vitro. Nanoscale Adv 1, 1472–1481.

(35). Chen YS, Zhao Y, Yoon SJ, Gambhir SS, and Emelianov S (2019) Miniature gold nanorods for photoacoustic molecular imaging in the second near-infrared optical window. Nat. Nanotechnol 14, 810–810. [PubMed: 31289408]

(36). Li JC, Hu Y, Yang J, Wei P, Sun WJ, Shen MW, Zhang GX, and Shi XY (2015) Hyaluronic acid-modified Fe_3O_4@au core/shell nanostars for multimodal imaging and photothermal therapy of tumors. Biomaterials 38, 10–21. [PubMed: 25457979]

(37). Pohling C, Campbell JL, Larson TA, Van de Sompel D, Levi J, Bachmann MH, Bohndiek SE, Jokerst JV, and Gambhir SS (2018) Smart-dust-nanorice for enhancement of endogenous raman signal, contrast in photoacoustic imaging, and T2-shortening in magnetic resonance imaging. Small 14.

(38). Xie XP, Liao JF, Shao XR, Li QS, and Lin YF (2017) The effect of shape on cellular uptake of gold nanoparticles in the forms of stars, rods, and triangles. Sci. Rep 7.

(39). Si P, Yuan E, Liba O, Winetraub Y, Yousefi S, SoRelle ED, Yecies DW, Dutta R, and de la Zerda A (2018) Gold nanoprisms as optical coherence tomography contrast agents in the second near-infrared window for enhanced angiography in live animals. ACS Nano 12, 11986–11994. [PubMed: 30422624]

(40). Neuschmelting V, Harmsen S, Beziere N, Lockau H, Hsu HT, Huang RM, Razansky D, Ntziachristos V, and Kircher MF (2018) Dual-modality surface-enhanced resonance raman scattering and multispectral optoacoustic tomography nanoparticle approach for brain tumor delineation. Small 14.

(41). Tian FR, Conde J, Bao CC, Chen YS, Curtin J, and Cui DX (2016) Gold nanostars for efficient in vitro and in vivo real-time SERS detection and drug delivery via plasmonic-tunable Raman/FTIR imaging. Biomaterials 106, 87–97. [PubMed: 27552319]

(42). Tang DY, Gao W, Yuan YJ, Guo LL, and Mei XF (2017) Novel biocompatible Au nanostars@PEG nanoparticles for in vivo CT imaging and renal clearance properties. Nanoscale Res. Lett 12.

(43). Zhao HY, Liu L, He J, Pan CC, Li H, Zhou ZY, Ding Y, Huo D, and Hu Y (2015) Synthesis and application of strawberry-like Fe_3O_4-Au nanoparticles as CT-MR dual-modality contrast agents in accurate detection of the progressive liver disease. Biomaterials 51, 194–207. [PubMed: 25771010]

(44). Cormode DP, Naha PC, and Fayad ZA (2014) Nanoparticle contrast agents for computed tomography: a focus on micelles. Contrast Media Mol. Imaging 9, 37–52. [PubMed: 24470293]

(45). Thaxton CS, Rink JS, Naha PC, and Cormode DP (2016) Lipoproteins and lipoprotein mimetics for imaging and drug delivery. Adv. Drug Delivery Rev 106, 116–131.

(46). Lin WJ, Zhang XF, Qian L, Yao N, Pan Y, and Zhang LJ (2017) Doxorubicin-loaded unimolecular micelle-stabilized gold nanoparticles as a theranostic nanoplatform for tumor-targeted chemotherapy and computed tomography imaging. Biomacromolecules 18, 3869–3880. [PubMed: 29032674]

(47). Wang YJ, Strohm EM, Sun Y, Wang ZX, Zheng YY, Wang ZG, and Kolios MC (2016) Biodegradable polymeric nanoparticles containing gold nanoparticles and paclitaxel for cancer

imaging and drug delivery using photoacoustic methods. Biomed. Opt. Express 7, 4125–4138. [PubMed: 27867720]

(48). Liu J, Cui T, and Ding Y (2018) Biomimetic gold nanoparticles. Compos. Commun 10, 209–216.

(49). Sun C, Yuan Y, Xu Z, Ji T, Tian Y, Wu S, Lei J, Li J, Gao N, and Nie G (2015) Fine-tuned h-ferritin nanocage with multiple gold clusters as near-infrared kidney specific targeting nanoprobe. Bioconjugate Chem 26, 193–196.

(50). Javed I, Sun YX, Adamcik J, Wang B, Kakinen A, Pilkington EH, Ding F, Mezzenga R, Davis TP, and Ke PC (2017) Cofibrillization of pathogenic and functional amyloid proteins with gold nanoparticles against amyloidogenesis. Biomacromolecules 18, 4316–4322. [PubMed: 29095600]

(51). Piao JG, Wang LM, Gao F, You YZ, Xiong YJ, and Yang LH (2014) Erythrocyte membrane is an alternative coating to polyethylene glycol for prolonging the circulation lifetime of gold nanocages for photothermal therapy. ACS Nano 8, 10414–10425. [PubMed: 25286086]

(52). Sun HP, Su JH, Meng QS, Yin Q, Chen LL, Gu WW, Zhang ZW, Yu HJ, Zhang PC, Wang SL, et al. (2017) Cancer cell membrane-coated gold nanocages with hyperthermia-triggered drug release and homotypic target inhibit growth and metastasis of breast cancer. Adv. Funct. Mater 27.

(53). Li Z, Peng HB, Liu JL, Tian Y, Yang WL, Yao JR, Shao ZZ, and Chen X (2018) Plant protein-directed synthesis of luminescent gold nanocluster hybrids for tumor imaging. ACS Appl. Mater. Interfaces 10, 83–90. [PubMed: 29220160]

(54). Jin J, Liu TT, Li MX, Yuan CX, Liu Y, Tang J, Feng ZQ, Zhou Y, Yang F, and Gu N (2018) Rapid in situ biosynthesis of gold nanoparticles in living platelets for multimodal biomedical imaging. Colloids Surf., B 163, 385–393.

(55). Liu TT, Li MX, Tang J, Li J, Zhou Y, Liu Y, Yang F, and Gu N (2019) An acoustic strategy for gold nanoparticle loading in platelets as biomimetic multifunctional carriers. J. Mater. Chem. B 7, 2138–2144. [PubMed: 32073572]

(56). Fesnak AD, June CH, and Levine BL (2016) Engineered T cells: the promise and challenges of cancer immunotherapy. Nat. Rev. Cancer 16, 566–581. [PubMed: 27550819]

(57). Lim WA, and June CH (2017) The principles of engineering immune cells to treat cancer. Cell 168, 724–740. [PubMed: 28187291]

(58). Murphy MB, Moncivais K, and Caplan AI (2013) Mesenchymal stem cells: environmentally responsive therapeutics for regenerative medicine. Exp. Mol. Med 45.

(59). Trounson A, and McDonald C (2015) Stem cell therapies in clinical trials: Progress and challenges. Cell Stem Cell 17, 11–22. [PubMed: 26140604]

(60). Villa C, Erratico S, Razini P, Fiori F, Rustichelli F, Torrente Y, and Belicchi M (2010) Stem cell tracking by nanotechnologies. Int. J. Mol. Sci 11, 1070–1081. [PubMed: 20480000]

(61). Kircher MF, Gambhir SS, and Grimm J (2011) Noninvasive cell-tracking methods. Nat. Rev. Clin. Oncol 8, 677–688. [PubMed: 21946842]

(62). Srivastava AK, and Bulte JWM (2014) Seeing stem cells at work in vivo. Stem Cell Rev. Rep 10, 127–144. [PubMed: 23975604]

(63). Xu CJ, Mu LY, Roes I, Miranda-Nieves D, Nahrendorf M, Ankrum JA, Zhao WA, and Karp JM (2011) Nanoparticle-based monitoring of cell therapy. Nanotechnology 22.

(64). Kim J, Chhour P, Hsu J, Litt HI, Ferrari VA, Popovtzer R, and Cormode DP (2017) Use of nanoparticle contrast agents for cell tracking with computed tomography. Bioconjugate Chem 28, 1581–1597.

(65). Chithrani BD, Ghazani AA, and Chan WCW (2006) Determining the size and shape dependence of gold nanoparticle uptake into mammalian cells. Nano Lett 6, 662–668. [PubMed: 16608261]

(66). Jiang Y, Huo SD, Mizuhara T, Das R, Lee YW, Hou S, Moyano DF, Duncan B, Liang XJ, and Rotello VM (2015) The interplay of size and surface functionality on the cellular uptake of sub-10 nm gold nanoparticles. ACS Nano 9, 9986–9993. [PubMed: 26435075]

(67). Shilo M, Sharon A, Baranes K, Motiei M, Lellouche JPM, and Popovtzer R (2015) The effect of nanoparticle size on the probability to cross the blood-brain barrier: an in-vitro endothelial cell model. J. Nanobiotechnol 13.

(68). Wong AC, and Wright DW (2016) Size-dependent cellular uptake of DNA functionalized gold nanoparticles. Small 12, 5592–5600. [PubMed: 27562251]

(69). Chhour P, Kim J, Benardo B, Tovar A, Mian S, Litt HI, Ferrari VA, and Cormode DP (2017) Effect of gold nanoparticle size and coating on labeling monocytes for CT tracking. Bioconjugate Chem 28, 260–269.

(70). Betzer O, Meir R, Dreifuss T, Shamalov K, Motiei M, Shwartz A, Baranes K, Cohen CJ, Shraga-Heled N, Ofir R, et al. (2015) In-vitro optimization of nanoparticle-cell labeling protocols for in-vivo cell tracking applications. Sci. Rep 5.

(71). Sun X, Gamal M, Nold P, Said A, Chakraborty I, Pelaz B, Schmied F, von Puckler K, Figiel J, Zhao Y, et al. (2019) Tracking stem cells and macrophages with gold and iron oxide nanoparticles - the choice of the best suited particles. Appl. Mater. Today 15, 267–279.

(72). Chinen AB, Guan CXM, Ko CH, and Mirkin CA (2017) The impact of protein corona formation on the macrophage cellular uptake and biodistribution of spherical nucleic acids. Small 13.

(73). Melby ES, Lohse SE, Park JE, Vartanian AM, Putans RA, Abbott HB, Hamers RJ, Murphy CJ, and Pedersen JA (2017) Cascading effects of nanoparticle coatings: surface functionalization dictates the assemblage of complexed proteins and subsequent interaction with model cell membranes. ACS Nano 11, 5489–5499. [PubMed: 28482159]

(74). Mirshafiee V, Kim R, Park S, Mahmoudi M, and Kraft ML (2016) Impact of protein pre-coating on the protein corona composition and nanoparticle cellular uptake. Biomaterials 75, 295–304. [PubMed: 26513421]

(75). Obst K, Yealland G, Balzus B, Miceli E, Dimde M, Weise C, Eravci M, Bodmeier R, Haag R, Calderon M, et al. (2017) Protein corona formation on colloidal polymeric nanoparticles and polymeric nanogels: Impact on cellular uptake, toxicity, immunogenicity, and drug release properties. Biomacromolecules 18, 1762–1771. [PubMed: 28511014]

(76). Piella J, Bastus NG, and Puntes V (2017) Size-dependent protein-nanoparticle interactions in citrate-stabilized gold nanoparticles: The emergence of the protein corona. Bioconjugate Chem 28, 88–97.

(77). Saha K, Rahimi M, Yazdani M, Kim ST, Moyano DF, Hou S, Das R, Mout R, Rezaee F, Mahmoudi M, et al. (2016) Regulation of macrophage recognition through the interplay of nanoparticle surface functionality and protein corona. ACS Nano 10, 4421–4430. [PubMed: 27040442]

(78). Astolfo A, Qie FX, Kibleur A, Hao XJ, Menk RH, Arfelli F, Rigon L, Hinton TM, Wickramaratna M, Tan TW, et al. (2014) A simple way to track single gold-loaded alginate microcapsules using X-ray CT in small animal longitudinal studies. Nanomedicine (N. Y., NY, U. S.) 10, 1821–1828.

(79). Betzer O, Shwartz A, Motiei M, Kazimirsky G, Gispan I, Damti E, Brodie C, Yadid G, and Popovtzer R (2014) Nanoparticle-based CT imaging technique for longitudinal and quantitative stem cell tracking within the brain: application in neuropsychiatric disorders. ACS Nano 8, 9274–9285. [PubMed: 25133802]

(80). Chhour P, Naha PC, O'Neill SM, Litt HI, Reilly MP, Ferrari VA, and Cormode DP (2016) Labeling monocytes with gold nanoparticles to track their recruitment in atherosclerosis with computed tomography. Biomaterials 87, 93–103. [PubMed: 26914700]

(81). Meir R, Betzer O, Motiei M, Kronfeld N, Brodie C, and Popovtzer R (2017) Design principles for noninvasive, longitudinal and quantitative cell tracking with nanoparticle-based CT imaging. Nanomedicine (N. Y., NY, U. S.) 13, 421–429.

(82). Kim T, Lee N, Arifin DR, Shats I, Janowski M, Walczak P, Hyeon T, and Bulte JWM (2017) In vivo micro-CT imaging of human mesenchymal stem cells labeled with gold-poly-l-lysine nanocomplexes. Adv. Funct. Mater 27.

(83). Meir R, Shamalov K, Betzer O, Motiei M, Horovitz-Fried M, Yehuda R, Popovtzer A, Popovtzer R, and Cohen CJ (2015) Nanomedicine for cancer immunotherapy: tracking cancer-specific T-cells in vivo with gold nanoparticles and CT imaging. ACS Nano 9, 6363–6372. [PubMed: 26039633]

(84). Comenge J, Sharkey J, Fragueiro O, Wilm B, Brust M, Murray P, Levy R, and Plagge A (2018) Multimodal cell tracking from systemic administration to tumour growth by combining gold nanorods and reporter genes. eLife 7.

(85). Lee SB, Lee SW, Jeong SY, Yoon G, Cho SJ, Kim SK, Lee IK, Ahn BC, Lee J, and Jeon YH (2017) Engineering of radioiodine-labeled gold core shell nanoparticles as efficient nuclear medicine imaging agents for trafficking of dendritic cells. ACS Appl. Mater. Interfaces 9, 8480–8489. [PubMed: 28218511]

(86). Dutta R, Liba O, SoRelle ED, Winetraub Y, Ramani VC, Jeffrey SS, Sledge GW, and de la Zerda A (2019) Real-time detection of circulating tumor cells in living animals using functionalized large gold nanorods. Nano Lett 19, 2334–2342. [PubMed: 30895796]

(87). Cormode DP, Si-Mohamed S, Bar-Ness D, Sigovan M, Naha PC, Balegamire J, Lavenne F, Coulon P, Roessl E, Bartels M, et al. (2017) Multicolor spectral photon-counting computed tomography: in vivo dual contrast imaging with a high count rate scanner. Sci. Rep 7.

(88). Si-Mohamed S, Cormode DP, Bar-Ness D, Sigovan M, Naha PC, Langlois JB, Chalabreysse L, Coulon P, Blevis I, Roessl E, et al. (2017) Evaluation of spectral photon counting computed tomography k-edge imaging for determination of gold nanoparticle biodistribution in vivo. Nanoscale 9, 18246–18257. [PubMed: 28726968]

(89). Cheng ZL, Al Zaki A, Hui JZ, Muzykantov VR, and Tsourkas A (2012) Multifunctional nanoparticles: cost versus benefit of adding targeting and imaging capabilities. Science 338, 903–910. [PubMed: 23161990]

(90). Liang H, Zhang XB, Lv YF, Gong L, Wang RW, Zhu XY, Yang RH, and Tan WH (2014) Functional DNA-containing nanomaterials: Cellular applications in biosensing, imaging, and targeted therapy. Acc. Chem. Res 47, 1891–1901. [PubMed: 24780000]

(91). Liu J, Yu M, Zhou C, Yang S, Ning X, and Zheng J (2013) Passive tumor targeting of renal-clearable luminescent gold nanoparticles: long tumor retention and fast normal tissue clearance. J. Am. Chem. Soc 135, 4978–4981. [PubMed: 23506476]

(92). Brigger I, Dubernet C, and Couvreur P (2012) Nanoparticles in cancer therapy and diagnosis. Adv. Drug Delivery Rev 64, 24–36.

(93). Danhier F, Feron O, and Preat V (2010) To exploit the tumor microenvironment: passive and active tumor targeting of nanocarriers for anti-cancer drug delivery. J. Controlled Release 148, 135–146.

(94). Yu MX, and Zheng J (2015) Clearance pathways and tumor targeting of imaging nanoparticles. ACS Nano 9, 6655–6674. [PubMed: 26149184]

(95). Ashton JR, Clark DP, Moding EJ, Ghaghada K, Kirsch DG, West JL, and Badea CT (2014) Dual-energy micro-CT functional imaging of primary lung cancer in mice using gold and iodine nanoparticle contrast agents: a validation study. PLoS One 9.

(96). Sykes EA, Chen J, Zheng G, and Chan WCW (2014) Investigating the impact of nanoparticle size on active and passive tumor targeting efficiency. ACS Nano 8, 5696–5706. [PubMed: 24821383]

(97). Perrault SD, Walkey C, Jennings T, Fischer HC, and Chan WCW (2009) Mediating tumor targeting efficiency of nanoparticles through design. Nano Lett 9, 1909–1915. [PubMed: 19344179]

(98). Lai SF, Ko BH, Chien CC, Chang CJ, Yang SM, Chen HH, Petibois C, Hueng DY, Ka SM, Chen A, et al. (2015) Gold nanoparticles as multimodality imaging agents for brain gliomas. J. Nanobiotechnol 13.

(99). Sela H, Cohen H, Elia P, Zach R, Karpas Z, and Zeiri Y (2015) Spontaneous penetration of gold nanoparticles through the blood brain barrier (bbb). J. Nanobiotechnol 13.

(100). Smilowitz HM, Meyers A, Rahman K, Dyment NA, Sasso D, Xue C, Oliver DL, Lichtler A, Deng XM, Ridwan SM, et al. (2018) Intravenously-injected gold nanoparticles (AuNPs) access intracerebral F98 rat gliomas better than AuNPs infused directly into the tumor site by convection enhanced delivery. Int. J. Nanomed 13, 3937–3948.

(101). Elci SG, Jiang Y, Yan B, Kim ST, Saha K, Moyano DF, Tonga GY, Jackson LC, Rotello VM, and Vachet RW (2016) Surface charge controls the suborgan biodistributions of gold nanoparticles. ACS Nano 10, 5536–5542. [PubMed: 27164169]

(102). Yue J, Feliciano TJ, Li WL, Lee A, and Odom TW (2017) Gold nanoparticle size and shape effects on cellular uptake and intracellular distribution of SiRNA nanoconstructs. Bioconjugate Chem 28, 1791–1800.

(103). Tong X, Wang ZT, Sun XL, Song JB, Jacobson O, Niu G, Kiesewetter DO, and Chen XY (2016) Size dependent kinetics of gold nanorods in EPR mediated tumor delivery. Theranostics 6, 2039–2051. [PubMed: 27698939]

(104). Rahme K, Chen L, Hobbs RG, Morris MA, O'Driscoll C, and Holmes JD (2013) PEGylated gold nanoparticles: polymer quantification as a function of PEG lengths and nanoparticle dimensions. RSC Adv 3, 6085–6094.

(105). Wang J, Bai R, Yang R, Liu J, Tang JL, Liu Y, Li JY, Chai ZF, and Chen CY (2015) Size- and surface chemistry-dependent pharmacokinetics and tumor accumulation of engineered gold nanoparticles after intravenous administration. Metallomics 7, 516–524. [PubMed: 25671498]

(106). Wang S, Huang P, and Chen XY (2016) Hierarchical targeting strategy for enhanced tumor tissue accumulation/retention and cellular internalization. Adv. Mater 28, 7340–7364. [PubMed: 27255214]

(107). Huo SD, Chen SZ, Gong NQ, Liu J, Li XL, Zhao YY, and Liang XJ (2017) Ultrasmall gold nanoparticles behavior in vivo modulated by surface polyethylene glycol (PEG) grafting. Bioconjugate Chem 28, 239–243.

(108). Her S, Jaffray DA, and Allen C (2017) Gold nanoparticles for applications in cancer radiotherapy: mechanisms and recent advancements. Adv. Drug Delivery Rev 109, 84–101.

(109). Jing LJ, Liang XL, Deng ZJ, Feng SS, Li XD, Huang MM, Li CH, and Dai ZF (2014) Prussian blue coated gold nanoparticles for simultaneous photoacoustic/CT bimodal imaging and photothermal ablation of cancer. Biomaterials 35, 5814–5821. [PubMed: 24746962]

(110). Liu Y, Ashton JR, Moding EJ, Yuan HK, Register JK, Fales AM, Choi J, Whitley MJ, Zhao XG, Qi Y, et al. (2015) A plasmonic gold nanostar theranostic probe for in vivo tumor imaging and photothermal therapy. Theranostics 5, 946–960. [PubMed: 26155311]

(111). Yao CP, Zhang LW, Wang J, He YL, Xin J, Wang SJ, Xu H, and Zhang ZX (2016) Gold nanoparticle mediated phototherapy for cancer. J. Nanomater

(112). Farokhzad OC, and Langer R (2009) Impact of nanotechnology on drug delivery. ACS Nano 3, 16–20. [PubMed: 19206243]

(113). Kunjachan S, Pola R, Gremse F, Theek B, Ehling J, Moeckel D, Hermanns-Sachweh B, Pechar M, Ulbrich K, Hennink WE, et al. (2014) Passive versus active tumor targeting using RGD- and NGR-modified polymeric nanomedicines. Nano Lett 14, 972–981. [PubMed: 24422585]

(114). Ashton JR, Gottlin EB, Patz EF, West JL, and Badea CT (2018) A comparative analysis of EGFR-targeting antibodies for gold nanoparticle CT imaging of lung cancer. PLoS One 13.

(115). Qian YC, Qiu MT, Wu QQ, Tian YY, Zhang Y, Gu N, Li SY, Xu L, and Yin R (2014) Enhanced cytotoxic activity of Cetuximab in EGFR-positive lung cancer by conjugating with gold nanoparticles. Sci. Rep 4.

(116). Kubota T, Kuroda S, Kanaya N, Morihiro T, Aoyama K, Kakiuchi Y, Kikuchi S, Nishizaki M, Kagawa S, Tazawa H, et al. (2018) HER2-targeted gold nanoparticles potentially overcome resistance to Trastuzumab in gastric cancer. Nanomedicine (N. Y., NY, U. S.) 14, 1919–1929.

(117). Wang RZ, Luo Y, Yang SH, Lin J, Gao DM, Zhao Y, Liu JG, Shi XY, and Wang XL (2016) Hyaluronic acid-modified manganese-chelated dendrimer-entrapped gold nanoparticles for the targeted CT/MR dual-mode imaging of hepatocellular carcinoma. Sci. Rep 6.

(118). Dinish US, Song ZG, Ho CJH, Balasundaram G, Attia ABE, Lu XM, Tang BZ, Liu B, and Olivo M (2015) Single molecule with dual function on nanogold: biofunctionalized construct for in vivo photoacoustic imaging and SERS biosensing. Adv. Funct. Mater 25, 2316–2325.

(119). Dixit S, Novak T, Miller K, Zhu Y, Kenney ME, and Broome AM (2015) Transferrin receptor-targeted theranostic gold nanoparticles for photosensitizer delivery in brain tumors. Nanoscale 7, 1782–1790. [PubMed: 25519743]

(120). Kwon SP, Jeon S, Lee SH, Yoon HY, Ryu JH, Choi D, Kim JY, Kim J, Park JH, Kim DE, et al. (2018) Thrombin-activatable fluorescent peptide incorporated gold nanoparticles for dual optical/computed tomography thrombus imaging. Biomaterials 150, 125–136. [PubMed: 29035738]

(121). Meyers JD, Cheng Y, Broome AM, Agnes RS, Schluchter MD, Margevicius S, Wang XN, Kenney ME, Burda C, and Basilion JP (2015) Peptide-targeted gold nanoparticles for photodynamic therapy of brain cancer. Part. Part. Syst. Charact 32, 448–457. [PubMed: 25999665]

(122). Avvakumova S, Galbiati E, Sironi L, Locarno SA, Gambini L, Macchi C, Pandolfi L, Ruscica M, Magni P, Collini M, et al. (2016) Theranostic nanocages for imaging and photothermal therapy of prostate cancer cells by active targeting of neuropeptide-y receptor. Bioconjugate Chem 27, 2911–2922.

(123). Conde J, Bao CC, Tan YQ, Cui DX, Edelman ER, Azevedo HS, Byrne HJ, Artzi N, and Tian FR (2015) Dual targeted immunotherapy via in vivo delivery of biohybrid RNAi-peptide nanoparticles to tumor-associated macrophages and cancer cells. Adv. Funct. Mater 25, 4183–4194. [PubMed: 27340392]

(124). Kim JY, Ryu JH, Schellingerhout D, Sun IC, Lee SK, Jeon S, Kim J, Kwon IC, Nahrendorf M, Ahn CH, et al. (2015) Direct imaging of cerebral thromboemboli using computed tomography and fibrin-targeted gold nanoparticles. Theranostics 5, 1098–1114. [PubMed: 26199648]

(125). Miao QQ, and Pu KY (2016) Emerging designs of activatable photoacoustic probes for molecular imaging. Bioconjugate Chem 27, 2808–2823.

(126). van Duijnhoven SMJ, Robillard MS, Langereis S, and Grul H (2015) Bioresponsive probes for molecular imaging: concepts and in vivo applications. Contrast Media Mol. Imaging 10, 282–308. [PubMed: 25873263]

(127). Jiang X, Du B, and Zheng J (2019) Glutathione-mediated biotransformation in the liver modulates nanoparticle transport. Nat Nanotechnol 14, 874–882. [PubMed: 31308501]

(128). Li X, Kim J, Yoon J, and Chen XY (2017) Cancer-associated, stimuli-driven, turn on theranostics for multimodality imaging and therapy. Adv. Mater 29.

(129). Lyu Y, and Pu KY (2017) Recent advances of activatable molecular probes based on semiconducting polymer nanoparticles in sensing and imaging. Adv. Sci 4.

(130). Pelton M (2015) Modified spontaneous emission in nanophotonic structures. Nat. Photonics 9, 427–435.

(131). Gao PF, Li M, Zhang Y, Dong C, Zhang GM, Shi LH, Li G, Yuan MJ, and Shuang SM (2019) Facile, rapid one-pot synthesis of multifunctional gold nanoclusters for cell imaging, hydrogen sulfide detection and pH sensing. Talanta 197, 1–11. [PubMed: 30771909]

(132). Wu YT, Shanmugam C, Tseng WB, Hiseh MM, and Tseng WL (2016) A gold nanocluster-based fluorescent probe for simultaneous pH and temperature sensing and its application to cellular imaging and logic gates. Nanoscale 8, 11210–11216. [PubMed: 27182741]

(133). Deepagan VG, Kumar EKP, Suh YD, and Park JH (2018) PEGylated gold nanoprobe bearing the diselenide bond for ROS-responsive fluorescence imaging. Macromol. Res 26, 577–580.

(134). Ma YX, Wang Q, Zhu QY, Liu MY, Chen D, Han ZH, Zhang CY, Lv LW, and Gu YQ (2018) Dual fluorescence nanoconjugates for ratiometric detection of reactive oxygen species in inflammatory cells. J. Biophotonics 11.

(135). Zhang L, Zhou J, Ma FJ, Wang QB, Xu H, Ju HX, and Lei JP (2019) Single-sided competitive axial coordination of g-quadruplex/hemin as molecular switch for imaging intracellular nitric oxide. Chem. - Eur. J 25, 490–494. [PubMed: 30407667]

(136). Fu X, Fu X, Wang Q, Sheng L, Huang X, Ma MH, and Cai ZX (2017) Fluorescence switch biosensor based on quantum dots and gold nanoparticles for discriminative detection of lysozyme. Int. J. Biol. Macromol 103, 1155–1161. [PubMed: 28579467]

(137). Liu C, Li SY, Gu YJ, Xiong HH, Wong WT, and Sun L (2018) Multispectral photoacoustic imaging of tumor protease activity with a gold nanocage-based activatable probe. Mol. Imaging Biol 20, 919–929. [PubMed: 29736563]

(138). He XW, Zeng T, Li Z, Wang GL, and Ma N (2016) Catalytic molecular imaging of microRNA in living cells by DNA-programmed nanoparticle disassembly. Angew. Chem., Int. Ed 55, 3073–3076.

(139). Vilela P, Heuer-Jungemann A, El-Sagheer A, Brown T, Muskens OL, Smyth NR, and Kanaras AG (2018) Sensing of vimentin mRNA in 2D and 3D models of wounded skin using DNA-coated gold nanoparticles. Small 14.

(140). Yang YJ, Huang J, Yang XH, Quan K, Wang H, Ying L, Xie NL, Ou M, and Wang KM (2015) FRET nanoflares for intracellular mRNA detection: avoiding false positive signals and minimizing effects of system fluctuations. J. Am. Chem. Soc 137, 8340–8343. [PubMed: 26110466]

(141). Khandelwal P, Singh DK, Sadhu S, and Poddar P (2015) Study of the nucleation and growth of antibiotic labeled AuNPs and blue luminescent Au-8 quantum clusters for Hg^{2+} ion sensing, cellular imaging and antibacterial applications. Nanoscale 7, 19985–20002. [PubMed: 26564987]

(142). Lakkakula JR, Divakaran D, Thakur M, Kumawat MK, and Srivastava R (2018) Cyclodextrin-stabilized gold nanoclusters for bioimaging and selective label-free intracellular sensing of Co^{2+} ions. Sens. Actuators, B 262, 270–281.

(143). Hu B, Cheng RR, Liu XJ, Pan XH, Kong FP, Gao W, Xu KH, and Tang B (2016) A nanosensor for in vivo selenol imaging based on the formation of Au-Se bonds. Biomaterials 92, 81–89. [PubMed: 27043769]

(144). Liang JC, Xiong HY, Wang W, Wen W, Zhang XH, and Wang SF (2018) "Luminescent-off/on" sensing mechanism of antibiotic-capped gold nanoclusters to phosphate-containing metabolites and its antibacterial characteristics. Sens. Actuators, B 255, 2170–2178.

(145). Persi E, Duran-Frigola M, Damaghi M, Roush WR, Aloy P, Cleveland JL, Gillies RJ, and Ruppin E (2018) Systems analysis of intracellular pH vulnerabilities for cancer therapy. Nat. Commun 9.

(146). Cao Y, Qian RC, Li DW, and Long YT (2015) Raman/fluorescence dual-sensing and imaging of intracellular pH distribution. Chem. Commun 51, 17584–17587.

(147). Jaworska A, Jamieson LE, Malek K, Campbell CJ, Choo J, Chlopicki S, and Baranska M (2015) SERS-based monitoring of the intracellular pH in endothelial cells: the influence of the extracellular environment and tumour necrosis factor-alpha. Analyst 140, 2321–2329. [PubMed: 25485622]

(148). Li ZC, Xia L, Li GK, and Hu YL (2019) Raman spectroscopic imaging of pH values in cancerous tissue by using polyaniline@gold nanoparticles. Microchim. Acta 186.

(149). Puppulin L, Hosogi S, Sun HX, Matsuo K, Inui T, Kumamoto Y, Suzaki T, Tanaka H, and Marunaka Y (2018) Bioconjugation strategy for cell surface labelling with gold nanostructures designed for highly localized pH measurement. Nat. Commun 9.

(150). Yu KK, Li K, Qin HH, Zhou Q, Qian CH, Liu YH, and Yu XQ (2016) Construction of pH-sensitive "submarine" based on gold nanoparticles with double insurance for intracellular pH mapping, quantifying of whole cells and in vivo applications. ACS Appl. Mater. Interfaces 8, 22839–22848. [PubMed: 27532147]

(151). Liu XJ, Song XX, Luan DR, Hu B, Xu KH, and Tang B (2019) Real-time in situ visualizing of the sequential activation of caspase cascade using a multicolor gold-selenium bonding fluorescent nanoprobe. Anal. Chem 91, 5994–6002. [PubMed: 30942074]

(152). Musnier B, Wegner KD, Comby-Zerbino C, Trouillet V, Jourdan M, Hausler I, Antoine R, Coll JL, Resch-Genger U, and Le Guevel X (2019) High photoluminescence of shortwave infrared-emitting anisotropic surface charged gold nanoclusters. Nanoscale 11, 12092–12096. [PubMed: 31210229]

(153). Song JB, Huang P, and Chen XY (2016) Preparation of plasmonic vesicles from amphiphilic gold nanocrystals grafted with polymer brushes. Nat. Protoc 11, 2287–2299. [PubMed: 27763624]

(154). Song JB, Yang XY, Jacobson O, Lin LS, Huang P, Niu G, Ma QJ, and Chen XY (2015) Sequential drug release and enhanced photothermal and photoacoustic effect of hybrid reduced graphene oxide-loaded ultrasmall gold nanorod vesicles for cancer therapy. ACS Nano 9, 9199–9209. [PubMed: 26308265]

(155). Hu X, Li FY, Wang SY, Xia F, and Ling DS (2018) Biological stimulus-driven assembly/disassembly of functional nanoparticles for targeted delivery, controlled activation, and bioelimination. Adv. Healthcare Mater 7.

(156). Song JB, Lin LS, Yang Z, Zhu R, Zhou ZJ, Li ZW, Wang F, Chen JY, Yang HH, and Chen XY (2019) Self-assembled responsive bilayered vesicles with adjustable oxidative stress for enhanced cancer imaging and therapy. J. Am. Chem. Soc 141, 8158–8170. [PubMed: 31053030]

(157). Borglin J, Selegard R, Aili D, and Ericson MB (2017) Peptide functionalized gold nanoparticles as a stimuli responsive contrast medium in multiphoton microscopy. Nano Lett 17, 2102–2108. [PubMed: 28215085]

(158). Song J, Kim J, Hwang S, Jeon M, Jeong S, Kim C, and Kim S (2016) Smart gold nanoparticles for photoacoustic imaging: an imaging contrast agent responsive to the cancer microenvironment and signal amplification via pH-induced aggregation. Chem. Commun 52, 8287–8290.

(159). Gao XH, Yue Q, Liu ZN, Ke MJ, Zhou XY, Li SH, Zhang JP, Zhang R, Chen L, Mao Y, et al. (2017) Guiding brain-tumor surgery via blood-brain-barrier-permeable gold nanoprobes with acid-triggered MRI/SERS signals. Adv. Mater 29.

(160). Dai C, Yang CX, and Yan XP (2018) Self-quenched gold nanoclusters for turn-on fluorescence imaging of intracellular glutathione. Nano Res 11, 2488–2497.

(161). Bouche M, Puhringer M, Iturmendi A, Arnirshaghaghi A, Tsourkas A, Teasdale I, and Cormode DP (2019) Activatable hybrid polyphosphazene-AuNP nanoprobe for ROS detection by bimodal PA/CT imaging. ACS Appl. Mater. Interfaces 11, 28648–28656. [PubMed: 31321973]

(162). Wang PY, Bai YJ, Yao C, Li XM, Zhou L, Wang WX, El-Toni AM, Zi J, Zhao DY, Shi L, et al. (2017) Intracellular and in vivo cyanide mapping via surface plasmon spectroscopy of single Au-Ag nanoboxes. Anal. Chem 89, 2583–2591. [PubMed: 28192999]

(163). Chen ZX, Li JJ, Chen XQ, Cao JT, Zhang JR, Min QH, and Zhu JJ (2015) Single gold@silver nanoprobes for real-time tracing the entire autophagy process at single-cell level. J. Am. Chem. Soc 137, 1903–1908. [PubMed: 25606663]

(164). Kim T, Zhang QZ, Li J, Zhang LF, and Jokerst JV (2018) A gold/silver hybrid nanoparticle for treatment and photoacoustic imaging of bacterial infection. ACS Nano 12, 5615–5625. [PubMed: 29746090]

(165). Anselmo AC, and Mitragotri S (2016) Nanoparticles in the clinic. Bioeng. Transl. Med 1, 10–29. [PubMed: 29313004]

(166). Bobo D, Robinson KJ, Islam J, Thurecht KJ, and Corrie SR (2016) Nanoparticle-based medicines: a review of FDA-approved materials and clinical trials to date. Pharm. Res 33, 2373–2387. [PubMed: 27299311]

(167). Singh P, Pandit S, Mokkapati VRSS, Garg A, Ravikumar V, and Mijakovic I (2018) Gold nanoparticles in diagnostics and therapeutics for human cancer. Int. J. Mol. Sci 19.

(168). Leong HS, Butler KS, Brinker CJ, Azzawi M, Conlan S, Dufes C, Owen A, Rannard S, Scott C, Chen C, et al. (2019) On the issue of transparency and reproducibility in nanomedicine. Nat. Nanotechnol 14, 629–635. [PubMed: 31270452]

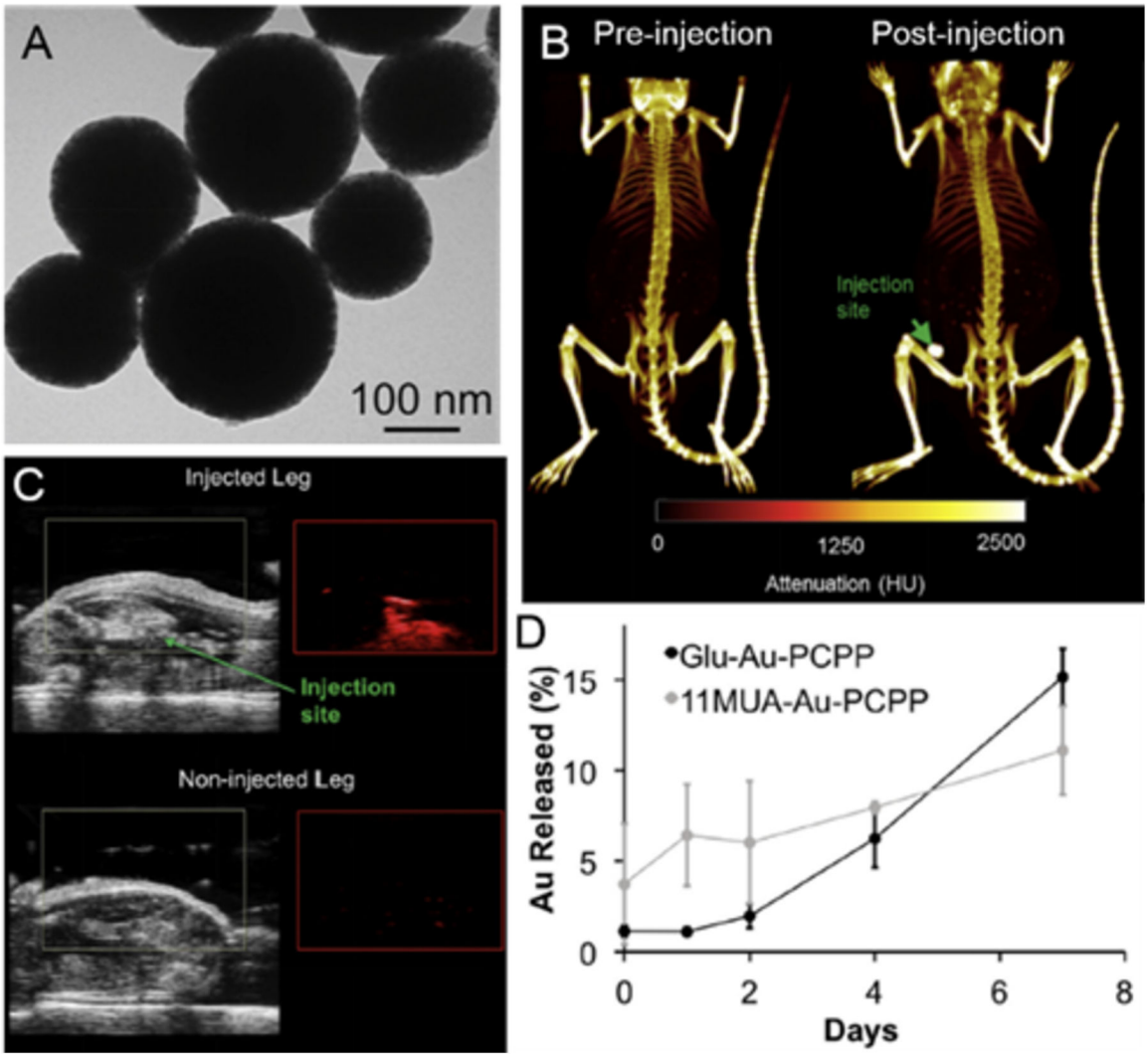

Figure 1.

A) TEM of biodegradable PCPP nanospheres loaded with small gold nanoparticles. *In vivo* imaging with B) CT and C) PAI. D) Degradation of PCPP nanospheres loaded with either glutathione-coated gold nanoparticles (Glu-Au-PCPP) or 11-mercaptoundecanoic acid (11MUA-Au-PCPP) in 10% serum at 37 °C. Adapted with permission from reference [9].

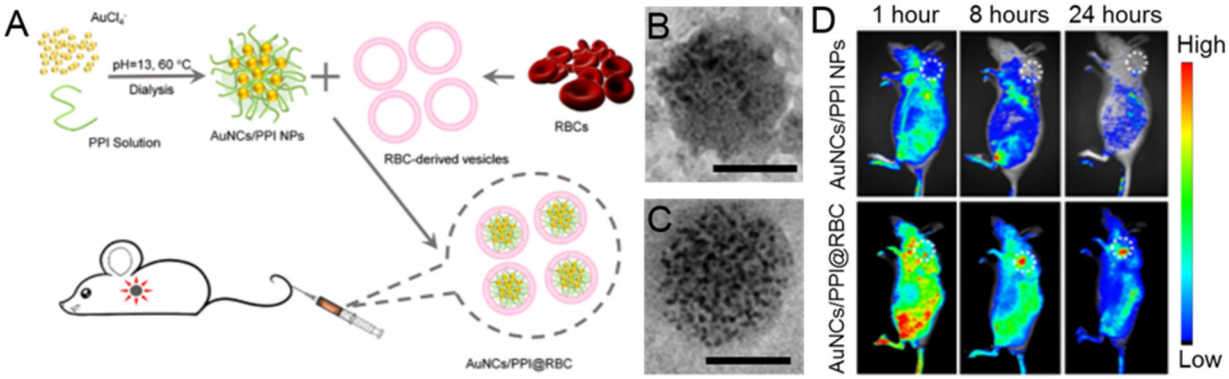

Figure 2.

A) Schematic for gold nano-assemblies preparation and subsequent *in vivo* fluorescence imaging. TEM micrographs of B) free AuNCs/PPI NPs and C) AuNC/PPI@RBC complexes. Scale bar = 50 nm. D) *In vivo* fluorescence imaging of mice injected with different nanoparticle formulations to show prolonged circulation time and enhanced tumor accumulation from RBC coated nanoparticles. Adapted with permission from reference [53].

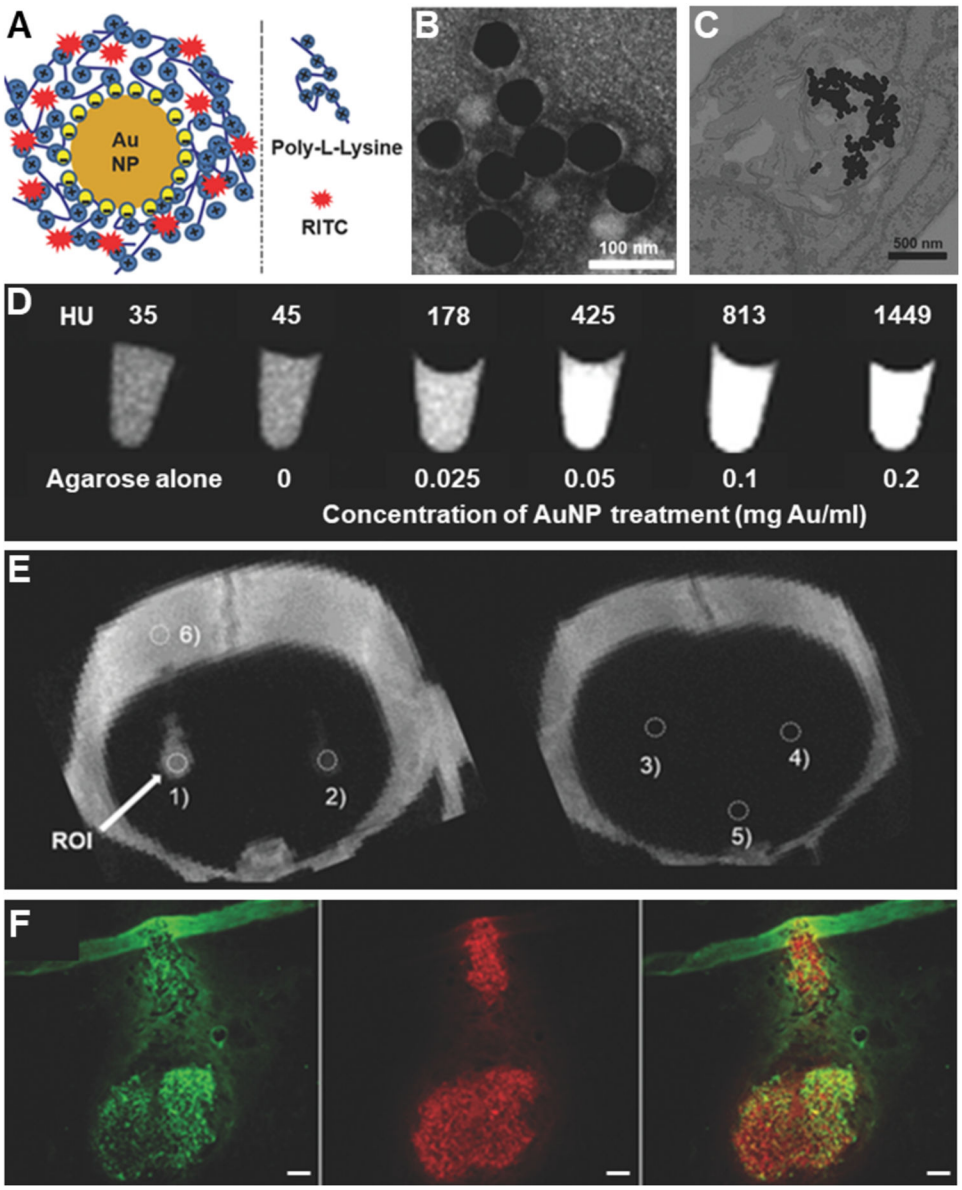

Figure 3.

A) Schematic depiction of AuNP-PLL complex. B) TEM of AuNP complexed with PLL and RITC. C) TEM of internalized AuNP in hMSC. D) *In vitro* microCT images of 1×10^6 hMSCs labeled with different concentration of AuNP-PLL complex. E) *In vivo* microCT images of labeled hMSCs injected in the striatum at different cell doses: (1) 5×10^5 cells, (2) 2×10^5 cells, (3) 6×10^4 cells, (4) 2×10^4 cells (HU = 76), (5) brain parenchyma, and (6) skull. F) Immunofluorescent images of the injection site (1) in panel (E). Left: transplanted hMSCs; middle: RITC in AuNP-PLL complex; right: overlay image of left and middle images. Scale bar = 200 μm. Adapted with permission from reference [82].

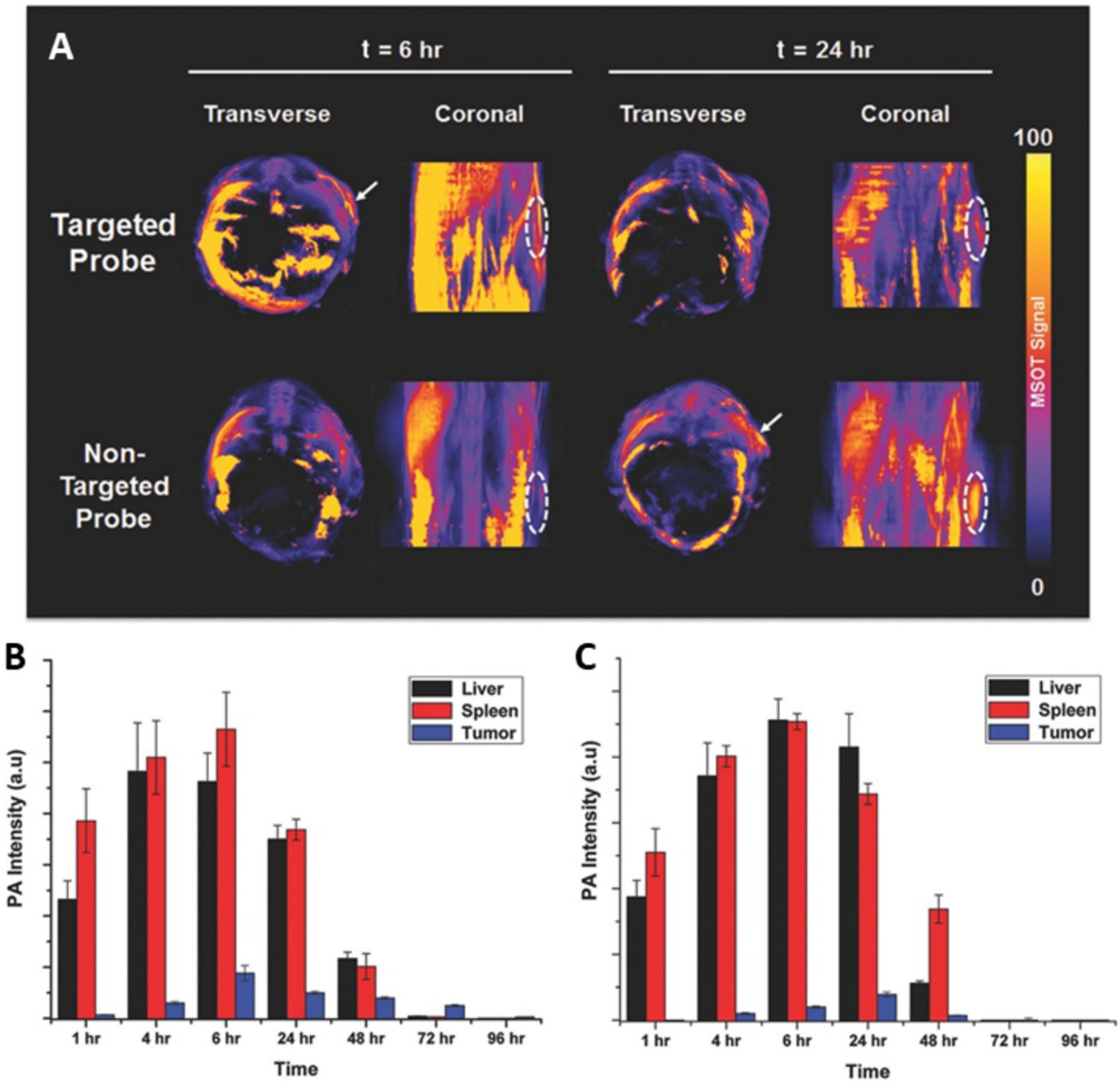

Figure 4.

A) *In vivo* non-background-corrected maximum intensity projection (MIP) PA images of a mouse at t = 6 and 24 h post-injection of both targeted and non-targeted AuNP. Corresponding PA signal intensity values at various time points from B) targeted AuNP and C) non-targeted AuNP. Adapted with permission from reference [118].

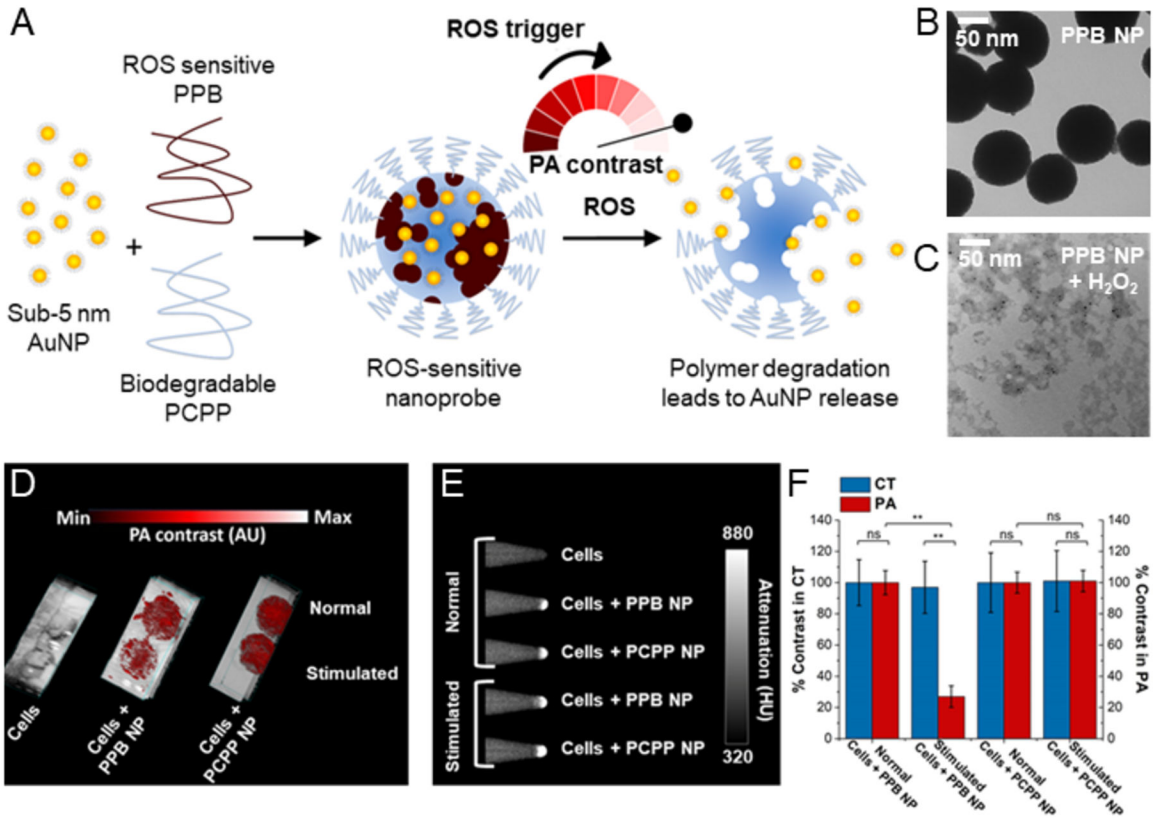

Figure 5.

A) Schematic of the production of plasmonic nanogels and their degradation triggered by ROS. Representative TEM images of the PPB NP B) maintaining their structure in H_2O, C) degraded upon exposure to H_2O_2. Influence of stimulation induced ROS overproduction in macrophages upon incubation with the ROS sensitive PPB NP and the control PCPP NP by D) PAI, E) CT contrast, F) contrast enhancement expressed as percentages in CT (blue) and PAI (red). Adapted with permission from reference [161].

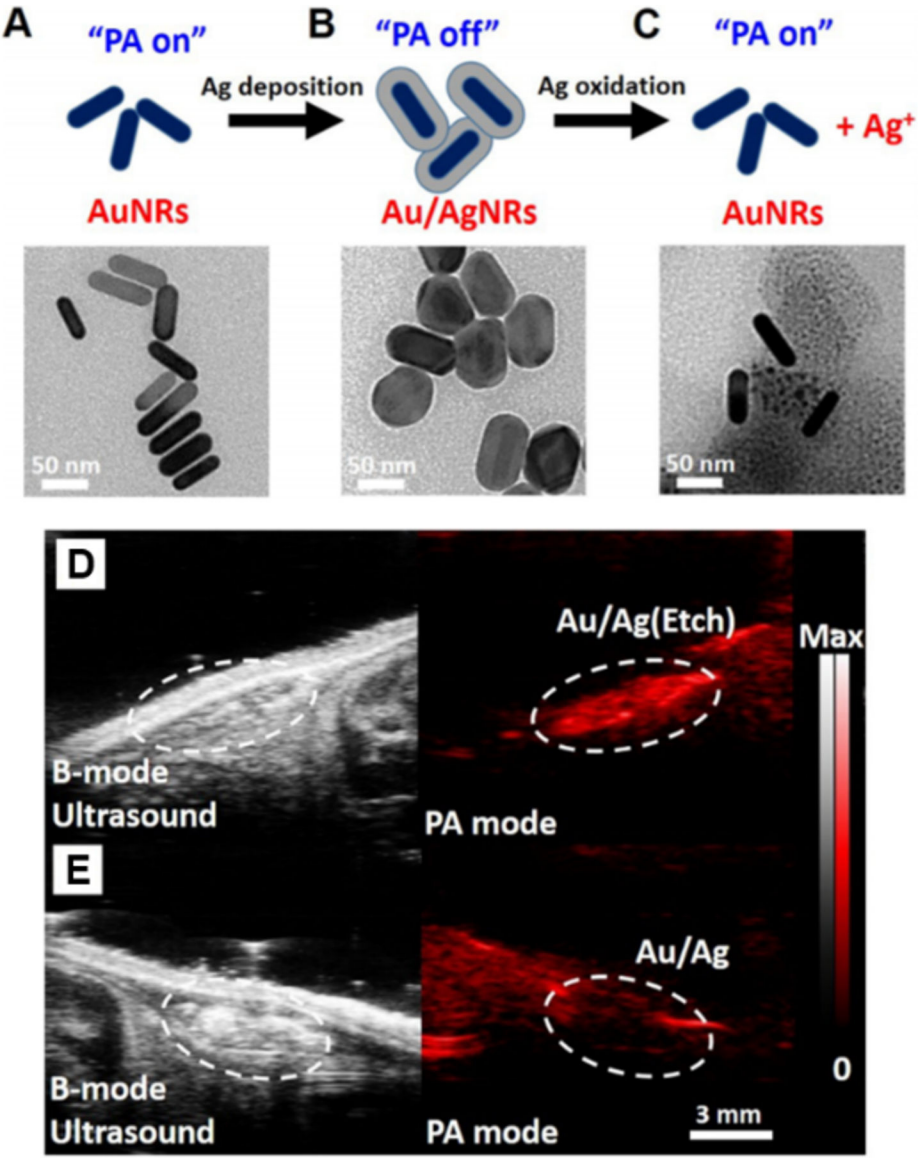

Figure 6.

Schematic and representative TEM images of A) synthesized AuNR, B) Au/AgNRs upon Ag deposition, C) AuNR following Ag^+ etching. Comparative ultrasound (gray scale) and photoacoustic (red scale) images of mice injected with D) Au/AgNR followed by silver etchant, and E) Au/AgNR. Adapted with permission from reference [164].